

OPTICAL TRANSITION RADIATION MEASUREMENTS OF THE LOS ALAMOS FREE ELECTRON LASER DRIVER

R. B. Fiorito and D. W. Rule  
 Naval Surface Warfare Center  
 White Oak, Silver Spring, MD 20903-5000

A.H. Lumpkin, R.B. Feldman, D.W. Feldman and B.E. Carlsten  
 Los Alamos National Laboratory  
 Los Alamos, NM 87545

Abstract

We have used the optical transition radiation (OTR) generated by the LANL FEL electron beam transiting a single mirrored quartz foil, and a two foil OTR interferometer, to measure the electron beam's divergence and spot size. Two gated intensified CID cameras are employed to simultaneously monitor the OTR's angular and spatial distributions. This method allows a determination of both the x and y emittances of the beam, when the beam is focused to an x or y waist, at a single position in the beam line. Both time integrated and time resolved measurements are possible with such a system. Time integrated results are compared with those obtained by measuring the beam spot size as a function of magnetic quadrupole focussing strength, which inherently requires multiple beam pulses.

Introduction

We describe recent results of optical transition radiation diagnostic experiments on the electron beam used to drive the Los Alamos free electron laser (FEL). To diagnose the beam, we have developed a time resolved imaging system which can simultaneously observe the spatial and angular distribution of optical transition radiation (OTR) produced by an electron beam impinging on one or two thin foils placed in the beam line. Proper analysis of these OTR images allows a determination of the current density distribution, beam divergence and energy of the electron beam producing the OTR.

A summary of the properties of OTR and its utility for measuring electron beam properties is given elsewhere<sup>1-4</sup>. Here we will only briefly review the key points. OTR is produced both in the forward and backward directions from a foil placed in the path of the electron beam, and has the unique feature that the backward pattern is centered on the direction of specular reflection of a ray coincident with the beam velocity vector. Figure 1 shows the patterns for normal and oblique incidence. As is readily apparent from the figure, it is experimentally very convenient to observe the backward OTR from a foil inclined at 45 degrees w.r.t. the beam axis. The pattern for a relativistic beam is a cone with opening angle equal to two divided by the Lorentz factor. Thus the angular position of the peak intensity of the radiation pattern from a single foil is a measure of the energy of the electron beam. The shape of the pattern can be used to determine the rms divergence of the beam. OTR is highly polarized in a plane formed by the velocity vector of the beam and the direction of observation. By observing the parallel and perpendicular components of the OTR separately, with the help of a polarizer, one can infer the beam divergence in two directions orthogonal to the beam axis.

OPTICAL TRANSITION RADIATION PATTERNS

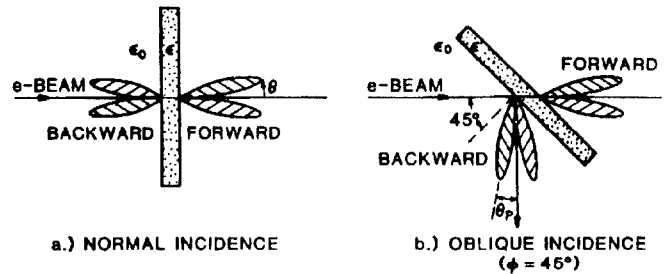


Fig. 1. Optical transition radiation patterns: a) normal incidence, b) oblique incidence.

By using a two foil system<sup>4</sup> (two parallel foils inclined at 45 degrees), the interference of the OTR patterns produced at each foil can be observed. Again, by means of a polarizer, the parallel and perpendicular intensity components can be observed separately. Theoretical interference patterns are given in Figure 2. Here the position of each fringe pair is a function of beam energy, and the visibility of the fringes is a function of beam divergence.

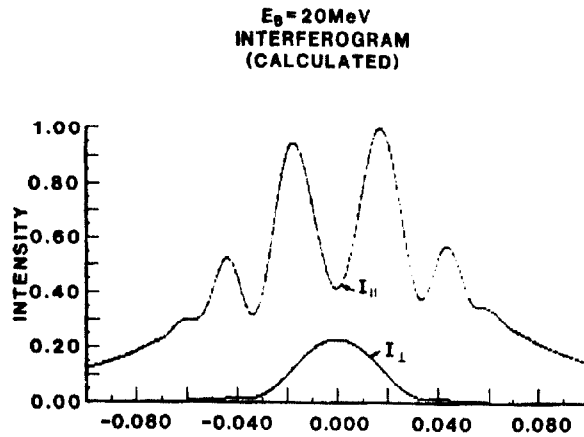


Fig. 2. OTR interferogram calculated for 20 Mev electron beam, interfoil spacing L=0.05 cm, wavelength=610 nm. The parallel and perpendicular components are shown for a divergence of 5.0 mrad.

We performed a series of experiments in which measurements of the LANL FEL electron beam emittance were made using two different methods. In one method

the OTR pattern and spatial distributions were measured simultaneously. In the other method the spatial distributions were observed and measured as a function of quadrupole focussing strength. The emittance obtained from these two methods is compared. The emittance of the beam can be obtained by setting the beam with the quadrupoles so as to form a waist in either the x or y direction (z is the e beam axis), and measuring divergence in the x-z or y-z plane.

### Experiments and Results

A schematic of the experimental arrangement is given in Figure 3. Two gated intensified CID cameras were used to capture the OTR images. One camera was focussed at the foil itself to monitor the spatial distribution of the OTR, and correspondingly, the distribution of the electron beam. The other camera is focussed at infinity and monitors the angular distribution of the OTR. The pattern resulting from the latter was used to measure the energy and divergence of the beam. A remotely controlled polarizer was placed in front of the lens to obtain perpendicular or parallel polarized OTR angular distributions.

### Schematic of OTR Experiment ( Los Alamos )

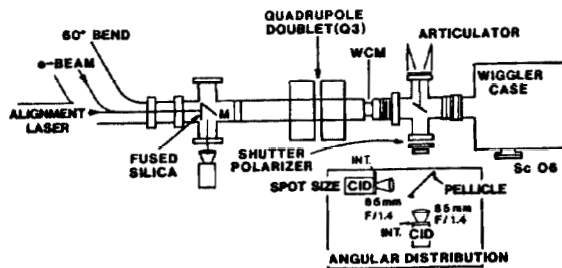


Fig. 3. Schematic of OTR experiment at Los Alamos.

Data were obtained just before the wiggler in the Los Alamos FEL. A 60 degree magnet triplet brings the 20 Mev electron beam onto the oscillator axis. Nominally we operated with about a 30 microsecond pulse, 46 ns micropulse spacing and ~ 1.2 nc/micropulse, with minimal magnetic bunching in the 60 degree bend. Our peak currents were about 50 A. Toward the end of the runs, the macropulse was lengthed to 100 microseconds and maximum bunching in the bend was increased to 10 ps. This increased the charge to 3 nc/micropulse. The corresponding peak and average current were 300 A. and 6 microamps respectively.

Figure 4 shows a composite picture and corresponding line scans of the two types of OTR images. The angular pattern shown is taken with a polarizer oriented parallel to the plane of incidence.

### Single Foil OTR Data

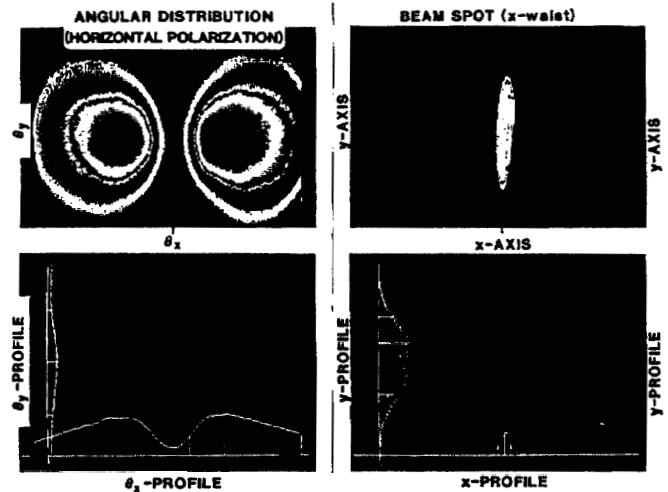


Fig. 4 Composite of OTR single foil data showing both divergence and beam spot images (upper) and line profiles (lower).

Figure 5 and 6 show the results of separately fitting scans of parallel and perpendicular OTR intensities. There is some ambiguity in these fits due to noise in the data images. This is especially true of the perpendicular intensity values which are much lower than the corresponding parallel intensity values, except in the vicinity of the center of the pattern. The parallel intensity data scan (Fig. 5) is taken at an x waist of the electron beam. The divergence for this position will be a maximum in the x-z plane. The fitted value is 4.9 mrad. Figure 6 shows a perpendicular intensity scan taken at an x waist as well. The fitted value for divergence in the y-z plane is 4.9 mrad also.

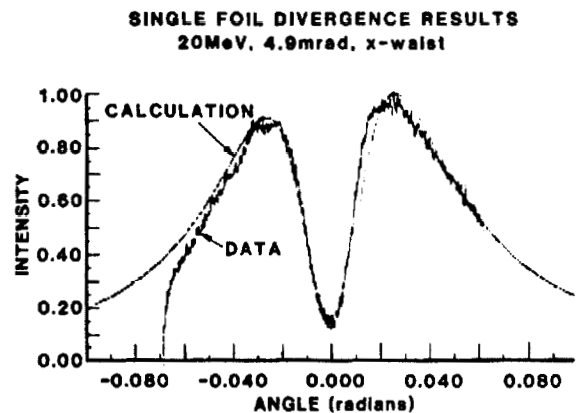


Fig. 5 Single foil data line scan of horizontally polarized OTR pattern compared with calculation using a divergence of 4.9 mrad.

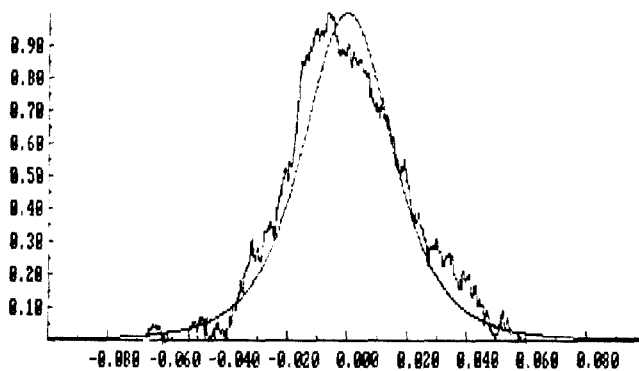


Fig. 6 Single foil data line scan of vertically polarized OTR pattern compared with calculation using a divergence of 4.9 mrad.

OTR interferograms were obtained using a two foil interferometer consisting of a 7.5 micron thick Kapton front foil separated by 0.5 mm from a thin aluminized quartz mirror, which serves as the second OTR foil. The interference pattern is observed through a 610 nm, 10 nm bandpass filter. The Kapton is more than 90% transmissive at this wavelength. It was noticed in imaging the beam spot, that a stray light source was observed at one end of the Kapton foil. The source of this light was most likely Cherenkov radiation trapped in the foil and channeled to the edge. The presence of this additional source of radiation caused an asymmetry in the OTR pattern which could be observed in a horizontal scan of a vertically polarized OTR pattern. In the presence of no background, only the perpendicular intensity contribution would be observed, and this would fall off rapidly from the center of the pattern as in Fig. 6. A subtraction of the perpendicular intensity component containing an asymmetric background contribution from a scan of parallel intensity can eliminate this contribution if it is not polarized, and therefore identical for both perpendicular and parallel intensities. This was done and the results are shown in Fig. 7, which shows a calculation of parallel minus perpendicular intensity compared to

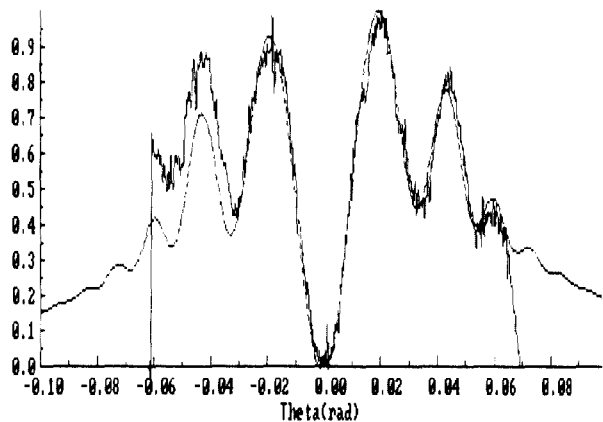


Fig. 7 Two foil OTR interferogram data of parallel minus perpendicular intensity compared to calculation using a projected beam divergence of 4 mrad in both the x-z and y-z planes.

measured data. A reasonably good fit is obtained using a divergence value of 4.0 mrad, except in the outermost fringes. The discrepancy may be due to partial polarization in the background, or clear foil amplitude contributions not presently included in the theory. We are looking into both of these possibilities.

### Discussion

We are in the process of a full comparison of beam divergence obtained by quadrupole focussing scans. In order to compare these two methods correctly one must compare true rms values for the beams spots, and then calculate the divergence in the x or y direction. Present analysis of the data obtained with the quadrupole focussing method, which simply uses the FWHM of the spot profile, yields divergences at the x and y beam waists. These values and corresponding beam radii give unnormalized x and y emittances of 1.8 pi mm mrad and 0.9 pi mm mrad respectively. The values obtained from OTR patterns yield unnormalized emittances of  $3.1 \pm 0.3$  and  $2.2 \pm 0.2$  pi mm mrad for x and y respectively. The difference between the results most likely is due to assumptions made in the analysis of the quadrupole data and is being reexamined. We are also presently analyzing simulation code results which predict the particle distribution in phase space as a function of axial distance. With knowledge of this function the rms divergence can be calculated at any position, in particular, at the OTR foil position. Also, the OTR pattern can be predicted by convolving the single or interference OTR pattern with the distribution function produced by the simulation.

### References

- [1] A. H. Lumpkin, et al, "Optical Transition Radiation Measurements for the Los Alamos and Boeing Free Electron Laser Experiments", Proc. of the Xth Intl. FEL Conf., Jerusalem, Israel, 1988.
- [2] R. B. Fiorito, et al, "Transition Radiation Diagnostics for Intense Charged Particle Beams", Proc. of the 6th Intl. Conf. on High Power Beams, Kobe, Japan, 1986.
- [3] D. W. Rule, "Transition Radiation Diagnostics for Intense Charged Particle Beams", Nucl. Instr. and Meth. B24/25, p. 901-904 (1987).
- [4] L. Wartski, et al, "Interference Phenomenon in Optical Transition Radiation and Its Application to Particle Beam Diagnostics and Multiple Scattering Measurements", J. Appl. Phys. 46, p. 3644 (1975).